Molecular and Cellular Endocrinology xxx (2014) xxx–xxx

Contents lists available at ScienceDirect

Molecular and Cellular Endocrinology

journal homepage: www.elsevier.com/locate/mce

A living biosensor model to dynamically trace glucocorticoid transcriptional activity during development and adult life in zebrafish

Francesca Benato [a,1], Elisa Colletti [a,1], Tatjana Skobo [a], Enrico Moro [b], Lorenzo Colombo [a], Francesco Argenton [a,*], Luisa Dalla Valle [a,*]

[a] Department of Biology, University of Padua, via U. Bassi 58/B, 35131 Padua, Italy
[b] Department of Molecular Medicine, University of Padua, via U. Bassi 58/B, 35131 Padua, Italy

ARTICLE INFO

Article history:
Received 14 November 2013
Received in revised form 24 April 2014
Accepted 24 April 2014
Available online xxxx

Keywords:
Zebrafish
Glucocorticoids
Dexamethasone
Glucocorticoid receptor
Reporter
Confocal microscopy

ABSTRACT

Glucocorticoids (GCs) modulate many cellular processes through the binding of the glucocorticoid receptor (GR) to specific responsive elements located upstream of the transcription starting site or within an intron of GC target genes. Here we describe a transgenic fish line harboring a construct with nine GC-responsive elements (GREs) upstream of a reporter (EGFP) coding sequence. Transgenic fish exhibit strong fluorescence in many known GC-responsive organs. Moreover, its enhanced sensitivity allowed the discovery of novel GC-responsive tissue compartments, such as fin, eyes, and otic vesicles. Long-term persistence of transgene expression is seen during adult stages in several organs. Pharmacological and genetic analysis demonstrates that the transgenic line is highly responsive to drug administration and molecular manipulation. Moreover, reporter expression is sensitively and dynamically modulated by the photoperiod, thus proving that these fish are an *in vivo* valuable platform to explore GC responsiveness to both endogenous and exogenous stimuli.

© 2014 Published by Elsevier Ireland Ltd.

1. Introduction

Glucocorticoids (GCs) are essential steroid hormones secreted by the adrenal cortex and the interrenal tissue of the head kidney in mammals and teleost fish, respectively, through a regulatory feedback loop under the control of the hypothalamic–pituitary–adrenal/interrenal (HPA/I) axis.

Cortisol is the main circulating GC both in teleosts and most mammals, including humans, while corticosterone is the major GC in rodents, amphibians, reptiles and birds (Bury and Sturm, 2007). GCs regulate many physiological processes, including intermediary metabolism, immune system, behavior and stress response (Sapolsky et al., 2000; Gross and Cidlowski, 2008). In mammals, GCs are also crucial for embryogenesis and development (Nesan and Vijayan, 2013). In the zebrafish, *Danio rerio*, unfertilized eggs and embryos during early stages of development have been shown to contain both cortisol and glucocorticoid receptor (*gr*) mRNAs (Alsop and Vijayan, 2008; Pikulkaew et al., 2010). The latter has been previously postulated to be essential for embryonic development, since its morpholino-mediated knockdown triggers several developmental defects, altered mesoderm patterning and limited survival of the embryos (Pikulkaew et al., 2011; Nesan et al., 2012).

The activation of the GC signaling pathway mainly depends on the binding to the cognate GC receptor, GR, a member of the nuclear receptor family of ligand-activated transcription factors, that is expressed in most tissues where it regulates tissue-specific sets of genes (Gross and Cidlowski, 2008; Chrousos and Kino, 2009). In the absence of ligand, GR is confined in the cytosol as part of a multiprotein complex that includes heat shock protein 70 (HSP70) and HSP90 (Rose et al., 2010). After GC binding, GR translocates into the nucleus, where it directly binds to GC responsive elements (GREs) in the promoter region of target genes or indirectly by means of protein–protein interactions with other DNA-binding proteins (Schoneveld et al., 2004; Rose et al., 2010).

An adult viable mutant zebrafish strain, named s357gr−/− has been recently identified (Ziv et al., 2013). In this mutant line, DNA binding activity of the receptor has been abolished by a single base-pair substitution in the DNA-binding domain leading to the replacement of an Arginine with a Cysteine (R443C). Gr-s357 mutants are viable, but show behavioral abnormalities, such as elevated startle response (Griffith et al., 2012) as well as a hyper-activated HPA axis (Ziv et al., 2013). Viability of larvae and

* Corresponding authors. Tel.: +39 049 827 6229; fax: +39 049 827 6300.
E-mail addresses: francesco.argenton@unipd.it (F. Argenton), luisa.dallavalle@unipd.it (L. Dalla Valle).
[1] The first and second authors contributed equally to this work.

http://dx.doi.org/10.1016/j.mce.2014.04.015
0303-7207/© 2014 Published by Elsevier Ireland Ltd.

Please cite this article in press as: Benato, F., et al. A living biosensor model to dynamically trace glucocorticoid transcriptional activity during development and adult life in zebrafish. Molecular and Cellular Endocrinology (2014), http://dx.doi.org/10.1016/j.mce.2014.04.015

UNCORRECTED PROOF

adult s357 homozygous mutants apparently contrasts with *gr*-MO knockdown results (Pikulkaew et al., 2011; Nesan et al., 2012). However, during early development, Gr-s357 homozygous mutants are supplied with GR protein and gr mRNA of maternal origin.

The GRE is shared by activated homodimerized receptors for GCs, mineralcorticoids, progesterone and androgens (Adler et al., 1992; Merkulov and Merkulova, 2009). It is composed of two imperfect palindromic, hexameric half-sites separated by a 3-nucleotide hinge (GGTACAnnnTGTTCT). A GR monomer binds first to the 3′-half-site, the most conserved one, followed by a second monomer that binds to the 5′-half-site, resulting in a DNA-bound GR dimer (Schoneveld et al., 2004). Alternatively, GR can work as a monomer bound only to the 3′-half-site (Merkulov and Merkulova, 2009).

To study GC activity a transgenic zebrafish line (GRE:Luc), in which four GRE tandem repeats drive luciferase reporter gene expression, has been recently developed (Weger et al., 2012). However, the GRE:Luc reporter gene allows less spatial resolution than that obtained by the green fluorescent protein (GFP) *in vivo* imaging (Hoffman, 2008). The advantage of using fluorescent proteins has been already shown in stable transgenic zebrafish lines, where the expression of reporter proteins is driven by responsive elements for different intracellular signaling pathways (Schwend et al., 2010; Laux et al., 2011; Gorelick and Halpern, 2011; Moro et al., 2012).

Hence, we here report the generation and validation of a stable transgenic zebrafish line in which Enhanced-GFP (EGFP) expression is driven by nine GRE tandem repeats. This line shows, in the absence of exogenous GCs, strong EGFP fluorescence starting with an ubiquitous pattern at early somitogenesis, and becoming mostly localized in brain and trunk muscles by 24 h post-fertilization (hpf). By 2–3 days post-fertilization (dpf), the fluorescence is detectable in well-known GC targets, such as liver, pancreas and intestine, and in new unpredicted tissues such as the cristae and lateral canals of the otic vesicles, scattered dermal mesenchymal-like cells and presumptive Kolmer-Agdur (KA″) interneurons, thus revealing novel GC targets.

This transgenic line (named ia20Tg following the Zebrafish Model Organism Database nomenclature) with enhanced sensitivity and spatial resolution represents a promising readout model to investigate the physiological functions of GC signaling *in vivo* during zebrafish development and adult life. Moreover, it may allow to study the circadian rhythm and modulation of neuronal and behavioral responses during feeding and stress as well as to detect compounds able to influence glucocorticoid-dependent responsiveness in pharmacological, toxicological and environmental research.

2. Materials and methods

2.1. Animals maintenance and handling

Zebrafish (*D. rerio*) were raised, staged and maintained according to standard protocols (Kimmel et al., 1995; Westerfield, 1995). Fish are kept in a 14 h light/10 h dark light cycle with light turning on at 8.00 am and off at 10.00 pm. For screening after 48 hpf and *in vivo* imaging, embryos and larvae were anesthetized with 0.04% tricaine (Westerfield, 1995). Analysis of light-dependent modulation of transgene reporter expression was performed in 5 dpf larvae starting from 2 h before light onset and collecting samples at 2 h interval for 28 h. The transgenic line Tg(12×Gli-HSV.Ul23:nlsmCherry)ia10 was used to localize the floor plate cells (Corallo et al., 2013). All live animals procedures were approved by the institutional ethics committee for animal testing (C.E.A.S.A.).

2.2. Generation of Tg(9×GCRE-HSV.Ul23:EGFP)ia20 reporter plasmid

To prepare the GRE reporter plasmid, we placed in tandem nine consensus GREs (TGTACAggaTGTTCT, with uppercase letters representing the GRE from the rat *tyrosine aminotransferase* promoter) (Grange et al., 1991). Briefly, we annealed and PCR amplified two phosphorylated oligonucleotides (5′-GTA GCT GAA CAT CCT GTA CAG GAT GTT CTA GC-3′ and 5′-GTA GCT AGA ACA TCC TGT ACA GCT CGA CGT AGC TAG AAC ATC CTG TAC A-3′; consensus GRE sequence is underlined), under the following reaction conditions: enzyme activation (Iproof High Fidelity PCR kit, Biorad, Milan, Italy) at 95 °C for 30 s followed by 40 cycles of denaturation (95 °C for 30 s), annealing (40 °C for 5 s) and extension (72 °C for 20 s). Reaction products were gel purified (Wizard® SV Gel and PCR Clean-Up System, Promega, Milan, Italy), ligated to one another using T4 DNA ligase (Promega) and cloned into pGEM-T Easy plasmid (Iproof High Fidelity PCR kit) pGEM®-T Easy Vector System, Promega). Nine GRE tandem repeats were PCR amplified (from a positive clone using two specific oligonucleotides (pGEM-GRE-F: 5′- *CCC***AAGCTT***GGG*TTCGATTGGATG-3′ with *Hind*III restriction site in bold letters and pGEM-GRE-R: 5′-*CCG***CTCGAG***CGG*TAGTGATTTAGC-3′ with *Xho*I restriction site in bold), purified (Wizard® SV Gel and PCR Clean-Up System, Promega), digested with *Hind*III and *Xho*I (Promega), gel purified, and ligated into the *Hind*III/*Bam*HI sites of the p5E-MCS vector from the Tol2 kit (Kwan et al., 2007) together with the *thymidine kinase* promoter (*tk*), retrieved by *Sal*I/*Bam*HI double digestion from PCR-blunt II-TOPO-*tk* (Moro et al., 2009).

Ligated 9×GRE-*tk* products were confirmed by sequencing. The resulting plasmid (p5E-9×GCRE-HSV.Ul23) was a 5′-entry clone suitable for the Gateway system. This clone, along with two Multisite Gateway-compatible entry vectors from the Tol2 kit (Kwan et al., 2007), a middle entry vector carrying the *egfp* open reading frame named pME-EGFP and a 3′-entry vector carrying a SV40 polyA tail from pCS2+(p3E-polyA), were incubated in the presence of the LR Clonase II Plus Enzyme mix (Invitrogen) and the destination vector pDestTol2pA2 as previously described (Kwan et al., 2007). The resulting destination plasmid contained a GRE-dependent EGFP reporter construct flanked by the minimal Tol2 transposon elements and was named Tg(9×GCRE-HSV.Ul23:EGFP) reporter plasmid. Reporter plasmid DNA (25–50 pg) was co-injected along with 25–50 pg of *in vitro* transcribed Tol2 *transposase* mRNA (Kawakami et al., 2004) into wild type (WT) 1-cell stage embryos.

2.3. Imaging

For confocal microscopy, transgenic embryos, larvae and adult tissues were embedded in 0.8% low-melting agarose and placed on a Petri capsule filled with fish water. The Nikon C2 confocal system was used to record images. WMISH-stained embryos were mounted in 87% glycerol in PBT or cleared and mounted in 2:1 benzyl benzoate/benzyl alcohol, observed under a Leica DMR microscope, and photographed with a Leica DC500 digital camera.

2.4. Drug treatments and microinjection of morpholinos (MOs)

Zebrafish transgenic embryos were incubated with different chemicals, all purchased from Sigma-Aldrich (Milan, Italy). All the chemicals were dissolved in ethanol to prepare stock solutions. Drug stocks were directly diluted 1:1000 in fish water (50×: 25 g Instant Ocean, 39.25 g $CaSO_4$, and 5 g $NaHCO_3$ for 1 l) to reach the desired final concentrations. Each treatment was performed in triplicate with 15 embryos per replica.

MO (Gene Tools, Philomath, OR) treatment was performed with gr^{ATG}MO (MO2-nr3c1), an antisense non-overlapping MO against

UNCORRECTED PROOF

Please cite this article in press as: Benato, F., et al. A living biosensor model to dynamically trace glucocorticoid transcriptional activity during development and adult life in zebrafish. Molecular and Cellular Endocrinology (2014), http://dx.doi.org/10.1016/j.mce.2014.04.015

the ATG translation initiation site of *gr* mRNA, *gr*^{splic}MO (MO4-nr3c1), a splice-site targeting MO as well as *gr*^{mism}MO (MO2-nr3c1-5m), as control MO, all previously described (Pikulkaew et al., 2011). For each MO, 8.2 ng were injected in the yolk of 1-cell stage embryos. Injections were performed under a dissecting microscope using a microinjector attached to a micromanipulator (Leica Microsystems, Milan, Italy). MO-injected embryos were then incubated in 1X fish water at 28.5 °C up to the desired stages of development.

2.5. Whole mount in situ hybridization (WMISH)

Zebrafish embryos were fixed overnight in 4% paraformaldehyde (PFA, Sigma) in phosphate-buffered saline (PBS) at the required stages of development. When necessary, pigmentation was removed by hydrogen peroxide treatment according to Thisse and Thisse (2008). WMISHs were performed as previously described by Thisse and Thisse (2008). All riboprobes for WMISHs are listed in Supplemental Table 1. After staining, the gr WMISH samples were sectioned in a vibratome (Leica VT1000S).

2.6. RNA extraction, reverse transcription and quantitative polymerase chain reaction (qPCR)

Total RNA was extracted from pools of 20–50 embryos, at the desired stages of development using TRIzol reagent (Invitrogen) and following the manufacturer's instructions. RNA samples were treated with DNAseI (DNA Free RNA kit, Zymo Rerearch) to eliminate possible genomic DNA contaminations, and stored at −80 °C until use.

For qPCR, 1 μg of total RNA derived from three different pools of embryos at each developmental stage was used for cDNA synthesis, with ThermoScriptTM RT–PCR system (Invitrogen, Carlsbad, CA) according to the manufacturer's protocol. qPCRs were performed with SYBR green method using a 7500 Real-Time PCR System (Applied Biosystems, Foster City, CA) and the GoTaq® qPCR Master Mix (Promega) following the manufacturer's protocol. The cycling parameters were 95 °C for 10 min, followed by 45 cycles at 95 °C for 30 s and 56 °C for 60 s. Threshold cycles (Ct) and dissociation curves were generated automatically by Applied Biosystems software. Sample Ct values were normalized with Ct values from zebrafish *elongation factor-1a* (*ef1a*), which was invariant in treated and control embryos at the same developmental stage. All analyses were performed in triplicate. The Relative Expression Software Tool 2009 (REST 2009) (Pfaffl et al., 2002) was used to estimate relative fold changes in the genes of interest, using a ratio of the Ct values and the PCR amplification efficiencies of the genes of interest and the housekeeping gene. REST 2009 uses randomization and bootstrapping methods to test the statistical significance of the gene expression ratios and calculate 95% confidence intervals for relative fold changes (Pfaffl, 2009). Significance of up-regulation of *egfp* expression with respect to *fkpb5* expression in the ia20 line response to pharmacological treatment with DEX was analyzed with GraphPad Prism Software. Primer sequences are reported in Supplemental Table 2.

3. Results

3.1. Generation of a GC-responsive transgenic zebrafish line and transgene expression analysis

In order to create a zebrafish model to analyze the *in vivo* GR-mediated GC activity, we assembled a transgenic construct containing nine consensus GREs upstream of a *thymidine kinase* (*tk*) minimal promoter [Herpes Simplex Virus (HSV) *thymidine kinase* gene (Ul23)] and the *egfp* coding sequence (Fig. 1A). The cassette obtained was used to generate the destination vector in the Tol2 transposon backbone (Kawakami, 2007). One-cell stage embryos were co-microinjected with the transgenic construct and *in vitro* transcribed Tol2 *transposase* mRNA. Transient EGFP expression was detected in many tissues of the injected embryos, such as liver, muscle and intestine. Six independent transgenic F0 chimeric founders were identified and crossed with wild-type (WT) fish to generate stable transgenic lines. F1 embryos from all the founders shared an identical EGFP expression pattern (data not shown), thus suggesting the independence of the degree of transgene expression from the genomic site of insertion. From this point onwards, we will use the nomenclature Tg(9×GCRE-HSV.Ul23:EGFP)ia20, (nicknamed ia20), to define the fish line used for all the described experiments.

To analyze the transgene expression pattern during development, F1 fish were outcrossed with WT fish. EGFP was detectable just after fertilization in the offspring of transgenic females mated with WT males (data not shown), while it was first visible from early somitogenesis (14 hpf) in the offspring of transgenic males crossed with WT females (Fig. 1C–C′). These results were validated by RT–PCR of *egfp* mRNA expression at 0, 1, 2, 3, 4, 5, 6, 7, 8, 16 and 24 hpf. Transgene transcripts were already detected at 0 hpf in the offspring of transgenic females, while they were evidenced by 2 hpf in the offspring of transgenic males. This result suggested that the *egfp* mRNA was maternally deposited in the ia20 line (Fig. 1B), whereas zygotic transcription of the transgene started by approximately 2 hpf, although levels were very low until 4 hpf.

The spatio-temporal expression of the reporter in the ia20 line was thoroughly analyzed during embryonic and early larval development by WMISH, fluorescence microscopy and confocal laser scanning microscopy. The analysis revealed that, in the absence of exogenous GC treatment, *egfp* mRNA and protein, first detected at 14 hpf, were more localized in the developing head, posterior trunk and tail bud (Fig. 1C–C′). This pattern of *gr* mRNA is similar to that previously observed at 15 hpf by WMISH (Pikulkaew et al., 2011). The shift in temporal reporter expression detected by RT–PCR, WMISH analyses and *in vivo* fluorescence microscopy was clearly due to the different sensitivity of the three techniques.

At 1 dpf, fluorescence was still strong in the head and showed an ascending gradient along the caudal trunk, with some intensity around the yolk sac and its extension (Fig. 1D). This expression pattern was confirmed by WMISH analysis of *egfp* mRNA (Fig. 1D′). At 3 dpf, fluorescence intensity in the head and tail regions declined to become more localized in internal organs at 6 dpf (Fig. 1E–E′–F–F′). For comparison, analyses of autofluorescence and EGFP expression in WT zebrafish embryos at the same developmental stages are reported on Supplemental Fig. 1.

Confocal microscopy analysis of 2- and 5-dpf larvae allowed a detailed localization of cells and tissues responding to endogenous GCs. At 2 dpf, EGFP signal was detected in known GC-target organs, such as olfactory bulbs and tracts (Fig. 2A), pituitary (Fig. 2B), liver (Fig. 2E), pronephros (Fig. 2F) and eye lens (not shown). Fluorescence was also detected in novel tissue domains, such as in the anterior and posterior cristae and, more feebly, the lateral canals of the otic vesicles (Fig. 2C), in mesenchymal-like cells of the skin (Fig. 2H) and, in the trunk, in two rows of cells located above the notochord and presenting the same organization of the KA″ interneurons (Huang et al., 2012) (Fig. 2G, Supplemental Fig. 2, Supplemental Video 1). The density of the latter cells was not uniform, but decreased going towards the posterior. At this stage, EGFP was also detected in the pectoral fin bud epidermis (Fig. 2D), where it co-localized with *fgf8a* mRNA (Supplemental Fig. 2). By 5 dpf, the reporter was still expressed in the above mentioned structures as well as in the heart (Fig. 2J), pancreas (Fig. 2K) and intestine (Fig. 2L). Notably, there is correspondence of *gr* expression and

UNCORRECTED PROOF

Please cite this article in press as: Benato, F., et al. A living biosensor model to dynamically trace glucocorticoid transcriptional activity during development and adult life in zebrafish. Molecular and Cellular Endocrinology (2014), http://dx.doi.org/10.1016/j.mce.2014.04.015

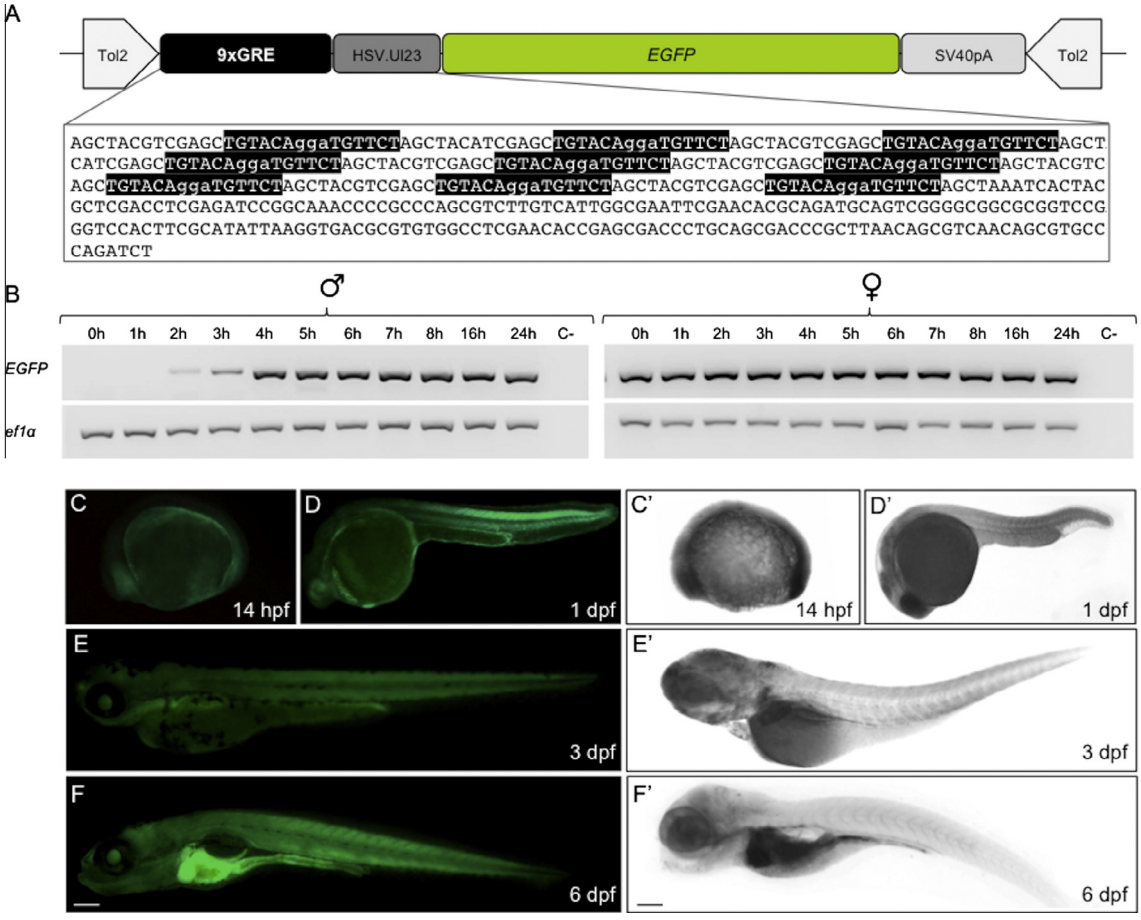

Fig. 1. Generation of the GRE-responsive line and developmental profile of GRE-mediated transcriptional activity of Tg(9×GCRE-HSV.UI23:EGFP)ia20 embryos and larvae (transgenic males crossed with WT females). (A) Schematic representation of the 9×GCRE-HSV.UI23:EGFP reporter construct designed in this study. The construct consists of a 0.45-kb fragment encoding nine repeating GREs (in black) from the rat *tyrosine aminotransferase* promoter (Grange et al., 1991) and a *thymidine kinase* (*tk*) promoter (HSV.UI23, in dark grey) inserted upstream of the *egfp* ORF (in green). The SV40 polyA signal (SV40pA in grey), which contains a transcriptional termination element, is directly downstream of the EGFP ORF and the entire element is flanked by Tol2 transposable elements. (B) RT–PCR analysis of *egfp* expression from the offspring of transgenic female or male and wild type mates at stages ranging from 0 up to 24 hpf. Expression of *ef1a* was used as a cDNA loading control. Fluorescence microscopy (C–F) and light microscopy (C′–F′) lateral views of zebrafish embryos and larvae at 14 hpf and 1, 3 and 6 dpf displaying the EGFP accumulation sites and the *egfp* mRNA localization during development. The protein and mRNA are first detectable at 14 hpf, when they both are ubiquitously distributed, with higher signals in the developing head and tail region (C–C′). The EGFP protein/mRNA localization remains the same by 1 dpf (D–D′), while it is visible in distinct domains, such as brain, liver and pronephros at 3 dpf (E–E′). By 6 dpf, the reporter expression is particularly intense in liver, intestine and pronephros (F–F′). Scale bar: 200 μM.

transgene activity as revealed by *gr* mRNA WMISH analysis performed on zebrafish embryos at the same stages reported on Fig. 1, as well as at 2 and 5 dpf (Supplemental Fig. 3).

3.2. The ia20 line responds to pharmacological treatment with GCs

To demonstrate the responsiveness of the transgenic line to exogenous GCs, transgenic males were outcrossed with WT females and the fluorescent offspring were treated at 48 hpf stage with nine different concentrations of the synthetic GC dexamethasone, DEX (10, 50, 100, 250 nM, 1, 2.5, 5, 10 and 25 μM) for 24 h. Larvae treated with 100 nM concentration of DEX or more, displayed, *in vivo*, a fluorescence intensification when compared to vehicle-treated controls. The increase was more evident with higher drug concentrations, with saturation of the response at 10 and 25 μM. This dose–response was also confirmed by WMISH (Fig. 3).

To verify whether the transgene was responding to the treatment with the GC agonist in a dose-dependent manner similar to that of an endogenous gene, qPCR analysis was carried out for *egfp* and *fkbp5* transcripts. The latter was selected because it is a sensitive biomarker of *in vivo* responses to GCs (Jääskeläinen et al., 2011). When compared to control, the expressions of the *egfp* and *fkbp5* transcripts were significantly higher with DEX treatment starting from 1 μM and 2.5 μM concentration, respectively (Fig. 3).

A more detailed analysis of the DEX-dependent responsiveness at the 10 μM concentration in the transgenic line was performed by confocal microscopy. A strong fluorescence enhancement with respect to control was detected in the pectoral fin epithelium (Supplemental Fig. 4A–A′), mesenchymal-like cells of the skin (Supplemental Fig. 4B–B′), skeletal muscle fibers (Supplemental Fig. 4C–C′), KA″ interneuron cells (Supplemental Fig. 4D–D′), as well as in the pituitary (Supplemental Fig. 4E–E′ and arrowhead in G′). EGFP signal also appeared in blood cells (Supplemental Fig. 4, arrows panel D′) and in the vessel endothelium (Supplemental Fig. 4, arrows in panel B′). Notably, in these cell types, the transgene was not expressed in the absence of GC agonist treatment. Moreover, with at least 10 μM DEX, a clear signal appeared also in the pineal gland (Supplemental Fig. 4F–F′ and arrow in panel G′). This localization was confirmed by double WMISH of *egfp* and *otx5* transcripts (Supplemental Fig. 2).

3.3. Selective response of the ia20 line to different steroids

A screening was carried out to evaluate responsiveness of the ia20 transgenic line to different steroids. All steroid treatments

Please cite this article in press as: Benato, F., et al. A living biosensor model to dynamically trace glucocorticoid transcriptional activity during development and adult life in zebrafish. Molecular and Cellular Endocrinology (2014), http://dx.doi.org/10.1016/j.mce.2014.04.015

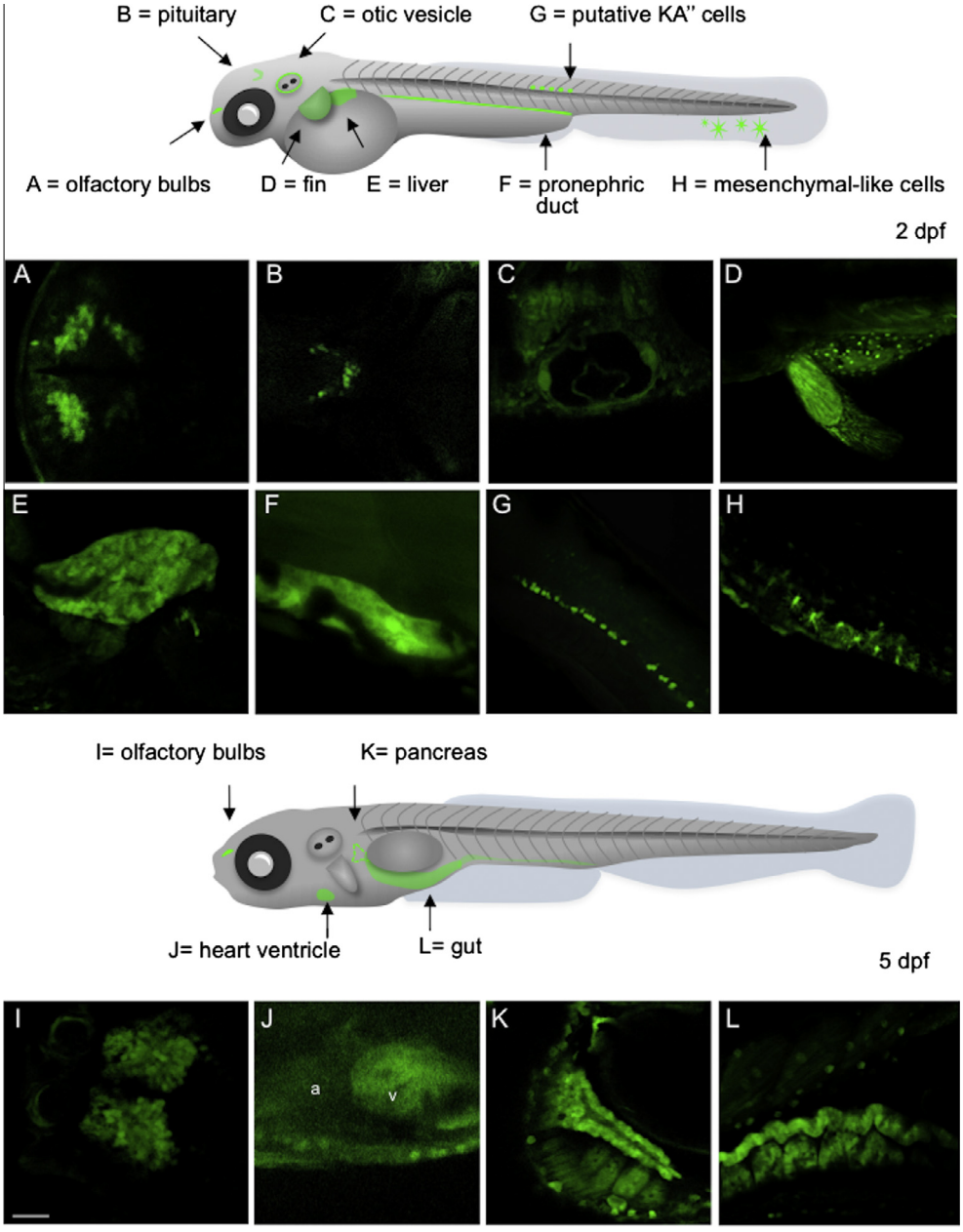

Fig. 2. Reporter expression in untreated 2- and 5-dpf transgenic zebrafish (transgenic males crossed with WT females). Top panel: schematic representation of a 2-dpf embryo indicating the EGFP positive cells and tissues. Below: 20× confocal microscopy pictures showing EGFP in olfactory bulbs and tracts (A, dorsal view), pituitary (B, dorsal view), otic vesicle (C, lateral view), pectoral fin (D, dorsal view), liver (E, lateral view), pronephros (F, lateral view), putative KA″ cells (G, lateral view) and dermal mesenchymal-like cells (H, lateral view). Bottom panel: schematic representation of a 5-dpf larva indicating the newly detectable EGFP-positive districts in addition to those already revealed at 2 dpf. Below: 20× confocal images showing fluorescence in the olfactory bulbs (I, dorsal view), heart (J, lateral view), pancreas (K, lateral view) and gut (L, lateral view). Scale bar: 200 μM.

(5 μM) started at 10 hpf and the effects on reporter expression were evaluated by WMISH at 1, 2 (not shown) and 3 dpf and by fluorescence microscopy analysis (Fig. 4). Incubation with cortisol led to the same results obtained with DEX: a sharp increase of *egfp* mRNA was already visible at 2 dpf in the same tissues. A modest effect on reporter activity was detected with corticosterone. The incubation with progesterone (see below in discussion) and prednisolone led to a clear increase of reporter transcription. Embryos treated with 11β-deoxycorticosterone (DOC), aldosterone, 11-ketotestosterone as well as 17β-estradiol displayed expression levels comparable to controls (Fig. 4).

Dose-dependent responsiveness of the transgenic line to five different concentrations (10 and 100 nM, 1, 5 and 25 μM) of cortisol, corticosterone and prednisolone were analyzed by qPCR of *egfp* and *fkbp5* transcripts. As reported in Supplemental Fig. 5 and in agreement with the WMISH results, the highest reporter induction was obtained with cortisol, followed by prednisolone and corticosterone. Moreover, the transgenic line appeared sensitive to low doses of prednisolone, as the corresponding *egfp* increase was statistically significant at 100 nM.

3.4. Reporter activity in ia20 fish decreases by GR knockdown and RU486 treatment

One-cell stage embryos were microinjected with three different MOs: gr^{ATG1}MO (MO2-nr3c1) to block the translation of both

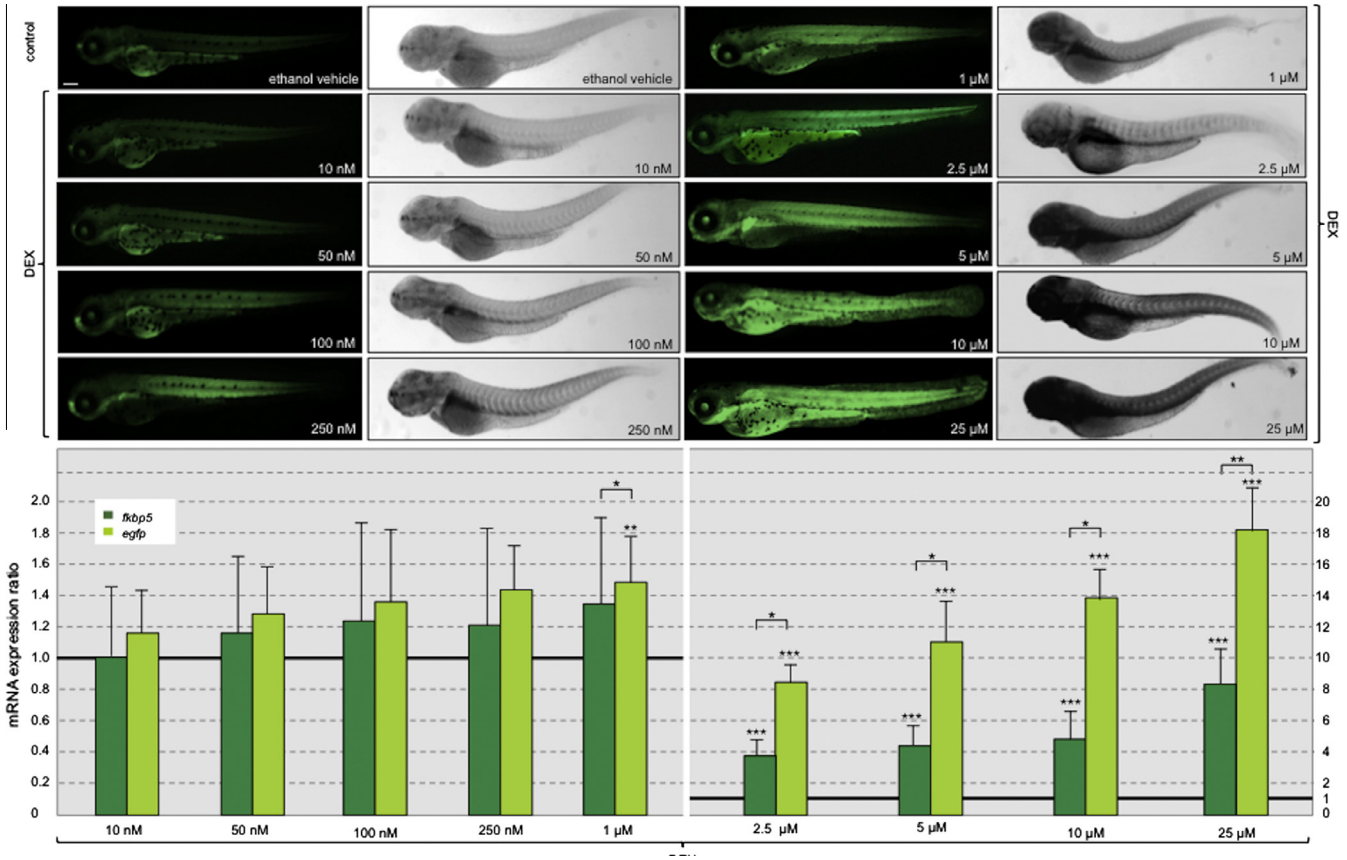

Fig. 3. DEX-induced fluorescence in Tg(9×GCRE-HSV.UI23:EGFP)ia20 zebrafish line is dose-dependent. Top panel: EGFP protein (on the left) and mRNA (on the right) distribution after treatment of transgenics with 10, 50, 100, 250 nM and 1, 2.5, 5, 10 and 25 µM DEX for 24 h as compared to their ethanol vehicle-treated siblings. Bottom panel: Fold changes in gene expression of *fkbp5* and *egfp*, in 10, 50, 100, 250 nM and 1, 2.5, 5, 10 and 25 µM DEX-treated transgenics compared to controls (set at 1) with vehicle only. The expression levels of the target genes were normalized on *ef1a* as housekeeping gene. The experiment was repeated three times with 10 embryos for each Q3 treatment. Values represent the mean ± S.E. Asterisks indicate that expression levels are significantly different from the control: $^{**}P < 0.01$, $^{***}P < 0.001$. Scale bar: 200 µM.

maternal and zygotic *gr* transcripts; gr^{splic}MO (MO4-nr3c1), a splicing MO to block post-transcriptionally the zygotic *gr* transcripts alone and gr^{mism}MO (MO2-nr3c1-5m), as a mismatched control MO. Morphants were incubated with or without 10 µM DEX for 24 h (from 2 to 3 dpf). The efficacy of gr^{ATG1}MO in targeting and blocking protein translation was determined in a previous work using an *in vitro* coupled transcription/translation coupled system, whereas the effectiveness of gr^{splic}MO was analyzed by RT–PCR (Pikulkaew et al., 2011).

The treatment with gr^{mism}MO did not modify either *egfp* or *fkbp5* transcription levels as assessed by qPCR (Fig. 5) confirming the presence of an active GR. Instead, microinjections with either gr^{ATG1}MO or gr^{splic}MO significantly reduced GC signaling as indicated by strong decrease of fluorescence and significant reduction of basal *fkbp5* gene expression. DEX treatment of the *gr*-morphants caused an increase of the *fkbp5* transcripts, suggesting incomplete penetrance of the two MOs. Analogously, the *egfp* transcripts were also increased by DEX treatment and this increase was statistically significant with respect to control (transgenic ia20 zebrafish without DEX) in gr^{splic}MO injected embryos (Fig. 5). Moreover, increase of both *egfp* and *fkbp5* transcripts after DEX treatment was statistically significant compared to *gr*-morphants. Finally, gr^{ATG1}MO treatment abolished completely or strongly reduced the fluorescence of transgenic fish in the target tissues for glucocorticoids previously shown in Fig. 2 (see Supplemental Fig. 6).

The specificity of transgene expression was further confirmed by treatment of embryos with DEX (10 µM) alone or together with the GR antagonist RU486 (50, 250 and 1250 nM) for 24 h (from 2 to 3 dpf). Co-treatment caused a significant and RU486 dose-dependent decrease of *egfp* and *fkbp5* mRNA levels compared to those in embryos treated with DEX alone (Fig. 6).

3.5. Adult fish of the ia20 line show endogenous GR transcriptional activity

In untreated adult males and females, transgene fluorescence was observed in many tissues, such as the esophageal sacs mucosa (Fig. 7A and K), ventricular epicardium (Fig. 7B and L), liver (Fig. 7C and M), intestinal mucosa (Fig. 7D and N), testis (Fig. 7E) and ovary (Fig. 7O). A lower fluorescence signal was also detected in the brain, skeletal muscle and kidney (not shown). After 24 h of 10 µM DEX treatment, both male and female transgenic fish showed an increase of the fluorescence in the brain, liver, intestinal mucosa and kidney (not shown) as well as detectable transgene expression in the skeletal elements of the splanchnocranium (Fig. 7H′ and R′), spinal cord (Fig. 7J′ and T′), eye (Fig. 7F′, G′, P′ and Q′) and skin (Fig. 7I′ and S′).

3.6. Transgene expression shows variations in tissues specificity and intensity with respect to the light cycle

Egfp transcription was analyzed by WMISH in 5-dpf transgenic larvae exposed to standard photoperiodic regimen (14 h light/10 h dark) at 2 h intervals starting from 2 h before light onset (8 am) for 28 h.

During the dark period, reporter activity was low and mainly limited to the digestive tract (from 20 pm to 6 am), but it increased just before the light onset (8 am), especially in the liver and intes-

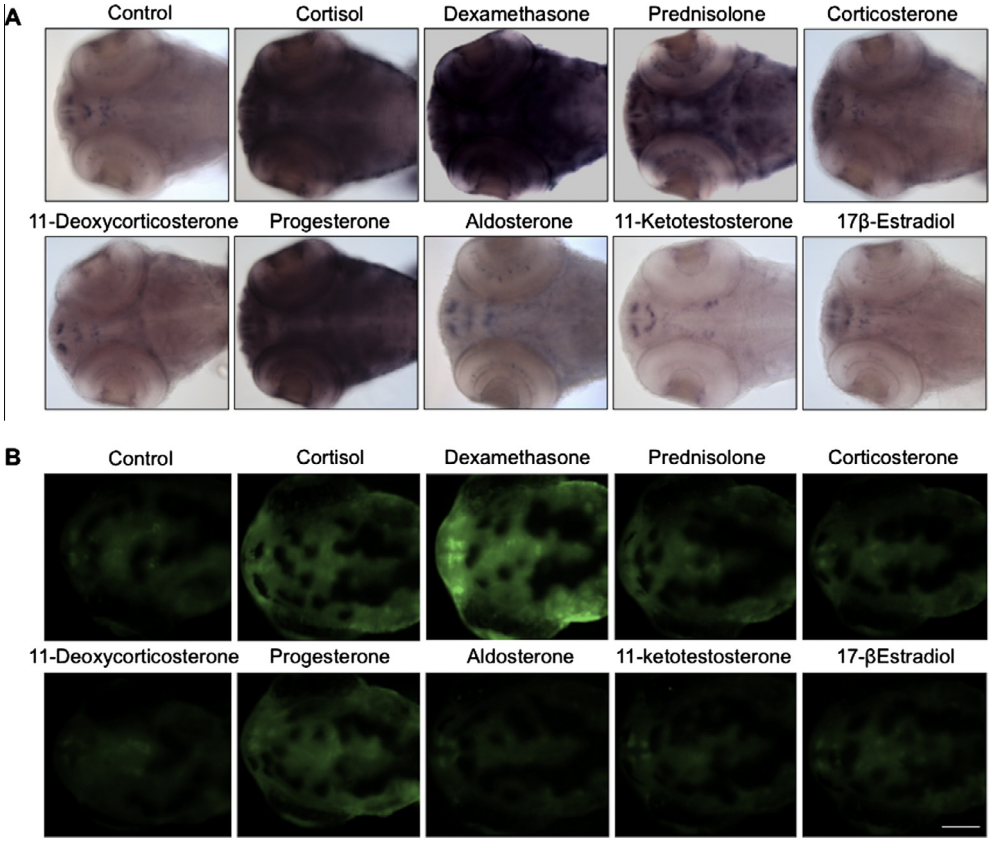

Fig. 4. Transgenic line responses to different steroid treatments. (A) Light microscopy dorsal view and (B) fluorescence microscopy images of 3-dpf transgenic zebrafish treated for 48 h with the indicated compounds. Responses were visualized by WMISH of *egfp* mRNA. Cortisol, dexamethasone, prednisolone, progesterone and corticosterone treatments increased reporter activity compared to control, while no changes were detectable with 11β-deoxycorticosterone (DOC), aldosterone, 11-ketotestosterone and 17β-estradiol (E2). Scale bar: 200 μM.

tine, where it remained high till 12 am to decrease later on (Fig. 8). In the eye and brain, the signal increased from 10 to 12 am, and then decreased. This expression pattern was confirmed by real time PCR of *egfp* and *fkbp5* transcripts at 5, 8 and 11 am, showing a significant up-regulation of both transcripts at 8 am (Supplemental Fig. 7). Moreover, the same expression pattern was obtained by WMISH for *fkbp5* expression in wild-type fish (Fig. 8). Fluorescence analysis of transgenic fish showed a similar circadian modulation of transgene expression with an EGFP signal delay consistent with the time required for translation (Fig. 8). Moreover, the decrease of fluorescence was slowed down due to the higher protein stability. Finally, WMISH of *gr* expression did not shown substantial variations during the LD cycle, as also reported by Dickmeis et al. (2007).

4. Discussion

In this work, we describe a transgenic zebrafish line in which the activation of the GC signaling pathway can be monitored *in vivo* in four dimensions. The integrated reporter transgene incorporates a conserved GRE tandem repeat that has been multiplied ninefold to increase cooperative binding of ligand-activated GR to GRE and boost transcription initiation of the *egfp* transgene (Jantzen et al., 1987). Analysis of the offspring generated by independent founders showed the same EGFP expression pattern, thus ruling out positional effects.

The transgenic line exhibits a high sensitivity, as evidenced by the detection of fluorescence in embryonic head and tail driven by endogenous GC already at 14 hpf. This favorably compares with a previously described transgenic reporter fish in which transcriptional activity, driven by fewer GRE tandem repeats, started at 1 dpf and only under DEX stimulation (Weger et al., 2012). Moreover, the use of a fluorescent molecule as reporter provides a higher spatial resolution, as shown by clear EGFP signaling in isolated dermal mesenchymal-like cells, blood and two rows of cells located above the notochord, possibly corresponding to the KA″ interneurons. These cells are distributed irregularly along the lateral floor plate domain and after differentiation lose the ability to respond to the Hedgehog (Hh) signal (Huang et al., 2012). This could explain the lack of total co-localization between GRE and Hh activity in the cells. The overall expression pattern is extended to all sites of potential GC activity (Pujols et al., 2002). Steroid selectivity of the reporter demonstrated high responsiveness to cortisol, DEX and prednisolone, low responsiveness to corticosterone, and ineffectiveness of mineralocorticoids, androgens and estrogens. The intense GRE-driven transcription induced by progesterone may be partly ascribed to its greater high cellular permeability as compared to GC and to the conversion of progesterone into cortisol. In fact the steroidogenic enzymes involved are already active in larvae, as demonstrated by a 90% reduction of cortisol concentrations in morphants of *cyp11a2*, at 72 hpf with respect to controls (Parajes et al., 2013). Moreover, progesterone responsiveness could also reflect some affinity of this steroid for GR, as reported in dog (Selman et al., 1996) and humans, where it acts as a low potency agonist (Koubovec et al., 2005). Interference by binding of progesterone to its specific receptor (PR) is unlikely because *pr* mRNA levels are very low till 2 dpf in zebrafish (Pikulkaew et al., 2010). The latter hypothesis was also excluded by incubating the *gr*-morphants (gr^{ATG1}MO and gr^{splic}MO) with 5 mμ progesterone

UNCORRECTED

Please cite this article in press as: Benato, F., et al. A living biosensor model to dynamically trace glucocorticoid transcriptional activity during development and adult life in zebrafish. Molecular and Cellular Endocrinology (2014), http://dx.doi.org/10.1016/j.mce.2014.04.015

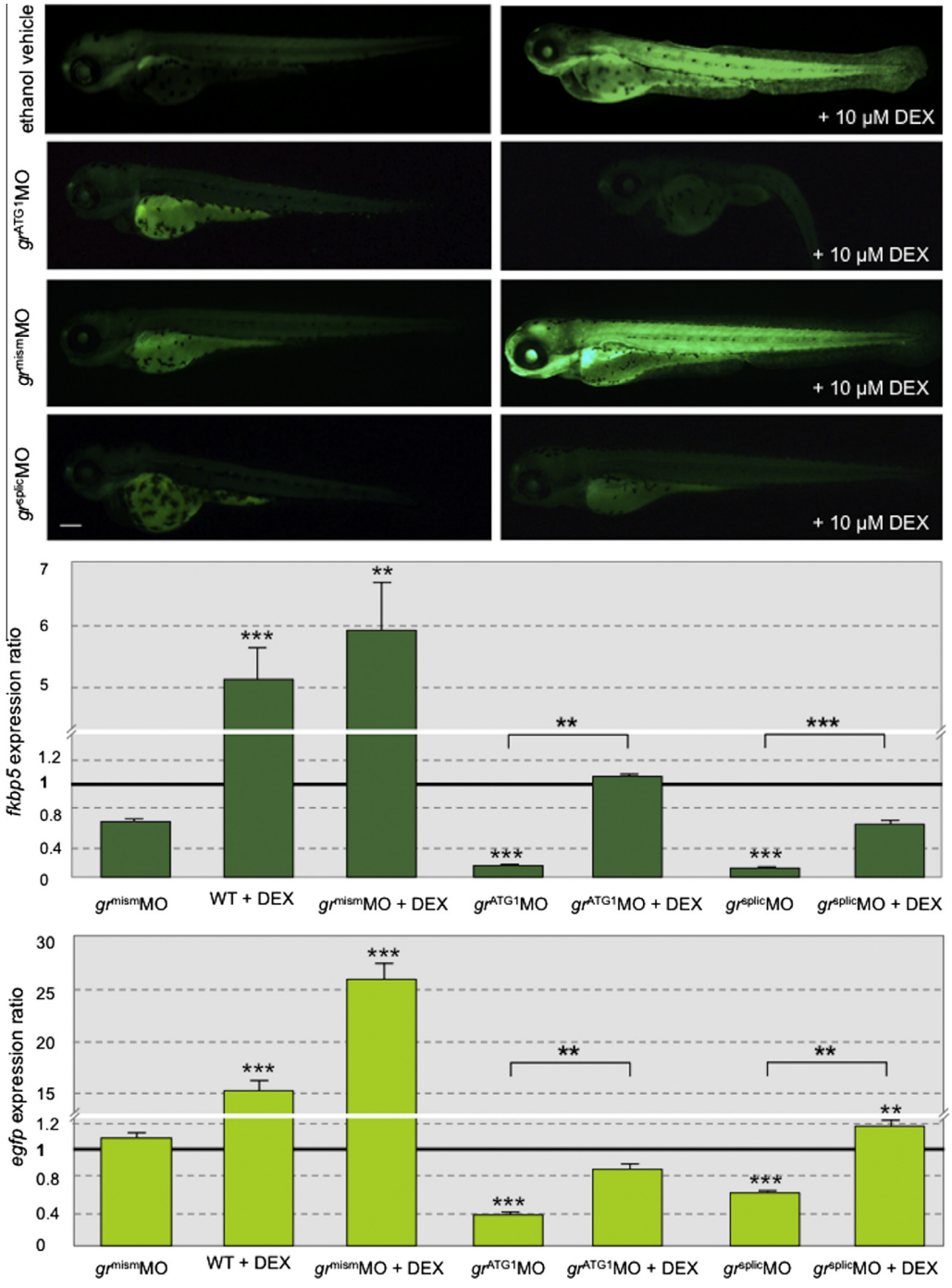

Fig. 5. Reduced GRE activity following *gr* MOs injections alone or combined with 10 μM DEX treatment of 2-dpf transgenics for 24 h. Top panel: EGFP protein localization in control (ia20 embryos) and after translation-blocking MO (gr^{ATG1}MO), missplicing MO (gr^{splic}MO) and mismatched control MO (gr^{mism}MO) injections alone (on the left) or combined with DEX treatment (on the right). Middle and bottom panels: fold changes in gene expression of *fkbp5* and *egfp* in embryos injected with gr^{mism}MO, gr^{ATG1}MO and gr^{splic}MO w/wo DEX treatment as compared to non- injected/non-treated control (set at 1). The expression levels of the target genes were normalized on *ef1a* as housekeeping gene. Values represent the mean ± S.E. Asterisks indicate expression levels that are significantly different from control (ia20 embryos) or between samples as indicated by the horizontal line: $^{**}P < 0.01$; $^{***}P < 0.001$. Scale bar: 200 μM.

(Supplemental Fig. 8). While in control fish the hormone treatment induced an increase of transgene activity, in gr-morphants we did not detect evident effects. Therefore, we validated the hypothesis that the progesterone effect was dependent on GR and, thus, on the metabolic conversion of progesterone to cortisol.

Dose-dependent responsiveness to DEX was shown after exposure to increasing DEX concentrations, concomitantly with enhanced expression of *egfp* and *fkbp5* mRNAs. Although the activity of GCs *in vivo* was normally enhanced using micromolar concentrations of DEX, as also reported for the GRE-Luc line (Weger et al., 2012), in the ia20Tg line the *egfp* mRNA increase, analyzed by qPCR, was statistically significant already at 1 μM. However, differences in the fluorescence levels and the hybridization signals were already appreciated at 100 nM of DEX. Similarly, signaling driven by endogenous GCs was highly amplified by adding DEX and the ia20 line has been found to respond in a

Please cite this article in press as: Benato, F., et al. A living biosensor model to dynamically trace glucocorticoid transcriptional activity during development and adult life in zebrafish. Molecular and Cellular Endocrinology (2014), http://dx.doi.org/10.1016/j.mce.2014.04.015

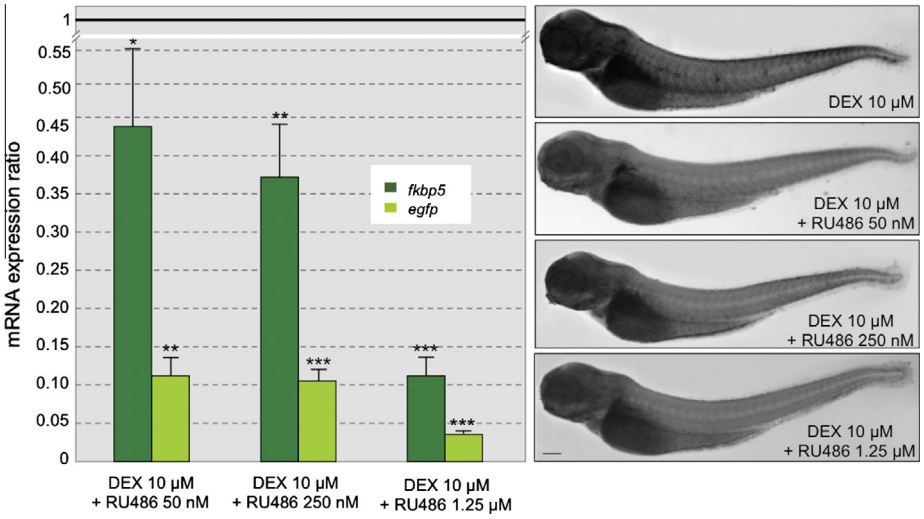

Fig. 6. Reduced GRE activity following treatment with the GR antagonist RU486. Two-dpf transgenic embryos were treated for 24 h with 10 µM DEX alone or combined with three different RU486 concentrations (50, 250 and 1250 nM). Left panel: fold changes in gene expression of *fkbp5* and *egfp* in treated embryos as compared to only DEX-treated control (set at 1). The expression levels of the target genes were normalized on *ef1a* as housekeeping gene. Values represent the mean ± S.E. Asterisks indicate expression levels that are significantly different from control (DEX-treated ia20): $^{*}P < 0.05$; $^{**}P < 0.01$; $^{***}P < 0.001$. Right panel: WMISH of *egfp* mRNA after DEX treatment alone or combined with RU486 at different concentrations. Scale bar: 200 µM.

dose-dependent manner also to GC agonists such as cortisol, prednisolone and corticosterone.

Knockdown of maternal and/or zygotic *gr* mRNAs determined a strong reduction of reporter activity induced by DEX and curtailed expressions of *egfp* and *fkbp5* mRNAs. The fact that these mRNAs were more reduced in morphant larvae not exposed to DEX suggests that DEX over-induced reporter activity, largely compensating for the knockdown effect. A similar decrease of fluorescence was obtained by co-treatment of transgenic embryos with the GR antagonist RU486 suggesting that, at early stages, the fish line is only reporting GC activity.

The similar modulation of *egfp* and *fkbp5* expression under different treatments is remarkable, because it demonstrates that, despite its artificial assemblage, the transgene is operating like an endogenous promoter. This matching, however, is only partial, because it does not cover indirect transactivation and transrepression due to crosstalk between GR and other transcription factors (Kassel and Herrlich, 2007), given the absence of additional docking sites for them in the transgene promoter. From a quantitative point of view, the increased number of responsive elements with respect to the ones located upstream to the *fkbp5* gene makes the transgene more prone to cooperativity and transcription, and the increased sensitivity enables the detection of new GC responsive targets, as the cristae and lateral canals of the otic vesicles, and scattered mesenchymal-like cells and putative KA″ cells.

Notably, we first detected an ascending rostro-caudal gradient of transgene, with the highest levels of GRE-reporter activity in the caudal portion of 24-hpf larvae. This expression pattern could be related to the key action of GR signaling in axial mesoderm development (Wang et al., 1999; Nesan et al., 2012). Interestingly, similarly to the well-known morphogen retinoic acid, also GCs play a function in modulating Wnt antagonists, in particular during differentiation of mesenchymal stem cells (Beildeck et al., 2010). Moreover, mouse skeletal development and mesenchymal progenitor cells are committed to osteoblastic lineage via a GC-dependent Wnt signaling (Zhou et al., 2009).

Relevant is our finding of localized transgene expression in the cardiac district of 2-dpf embryos and in the heart of 5-dpf larvae as well as in adult fish, where it is particularly intense in the ventricular epicardium. In mice, GC signaling is required for fetal heart maturation (Rog-Zielinska et al., 2013) and its over-activation through GR conditional expression perturbs adult cardiac physiology through conduction defects (Sainte-Marie et al., 2007). Given the persistence of transgene expression in the adult zebrafish heart, it is plausible that also in teleosts GC signaling plays a critical role in cardiomyocyte function and remodelling after insults, as shown in mice (De et al., 2011; Ren et al., 2012).

We also found that the esophageal sacs mucosa expressed, particularly at adulthood, a high level of reporter transgene. A key role of GC signaling in promoting cell proliferation and apoptosis in the esophageal epithelium was already demonstrated in medaka (Takagi et al., 2011). Moreover, adrenalectomy has been reported to result in reduced cell proliferation in the rat small intestine (Foligne et al., 2001). Pleiotropic effects of GCs have been proposed in the small intestine where, at least in mouse and human, an autonomous synthesis of these steroids has been recently documented (Mueller et al., 2007). In this organ, GCs are involved not only in the regulation of locally confined immune responses (Mueller et al., 2007), but also in intestinal cell maturation and transcriptional activation of genes involved in the absorptive function (Quaroni et al., 1999). Thus, it may be envisaged an involvement of GCs in tissue renewal and support of digestive function in the esophageal sacs and intestinal tract.

Fluorescence was observed also in the ovary of transgenic females. Confocal analysis of this organ demonstrated localized EGFP expression in follicular cells and in the ooplasmic and nuclear regions of developing oocytes. A modulation of ovarian functions by GCs as well as the presence of their receptor have been demonstrated in human (Rae et al., 2004), rat (Tetsuka et al., 1999) and teleost (Leatherland et al., 2010). Actually, fluorescence showed by ovulated oocytes and RT–PCR detection of maternal *egfp* mRNA starting from one-cell stage suggest the possibility of a continual activation of the GC signaling pathway throughout female gametogenesis.

On the other hand, *pr* transcripts and proteins have been found at high concentrations in zebrafish ovaries, both in follicular cells and early-stage oocytes (Hanna et al., 2010). Since the GRE sequence is shared as responsive element by the progesterone-PR complex, an involvement of the latter in transgene ovarian activation cannot be presently excluded. Similarly, given GRE

UNCORRECTED PROOF

Please cite this article in press as: Benato, F., et al. A living biosensor model to dynamically trace glucocorticoid transcriptional activity during development and adult life in zebrafish. Molecular and Cellular Endocrinology (2014), http://dx.doi.org/10.1016/j.mce.2014.04.015

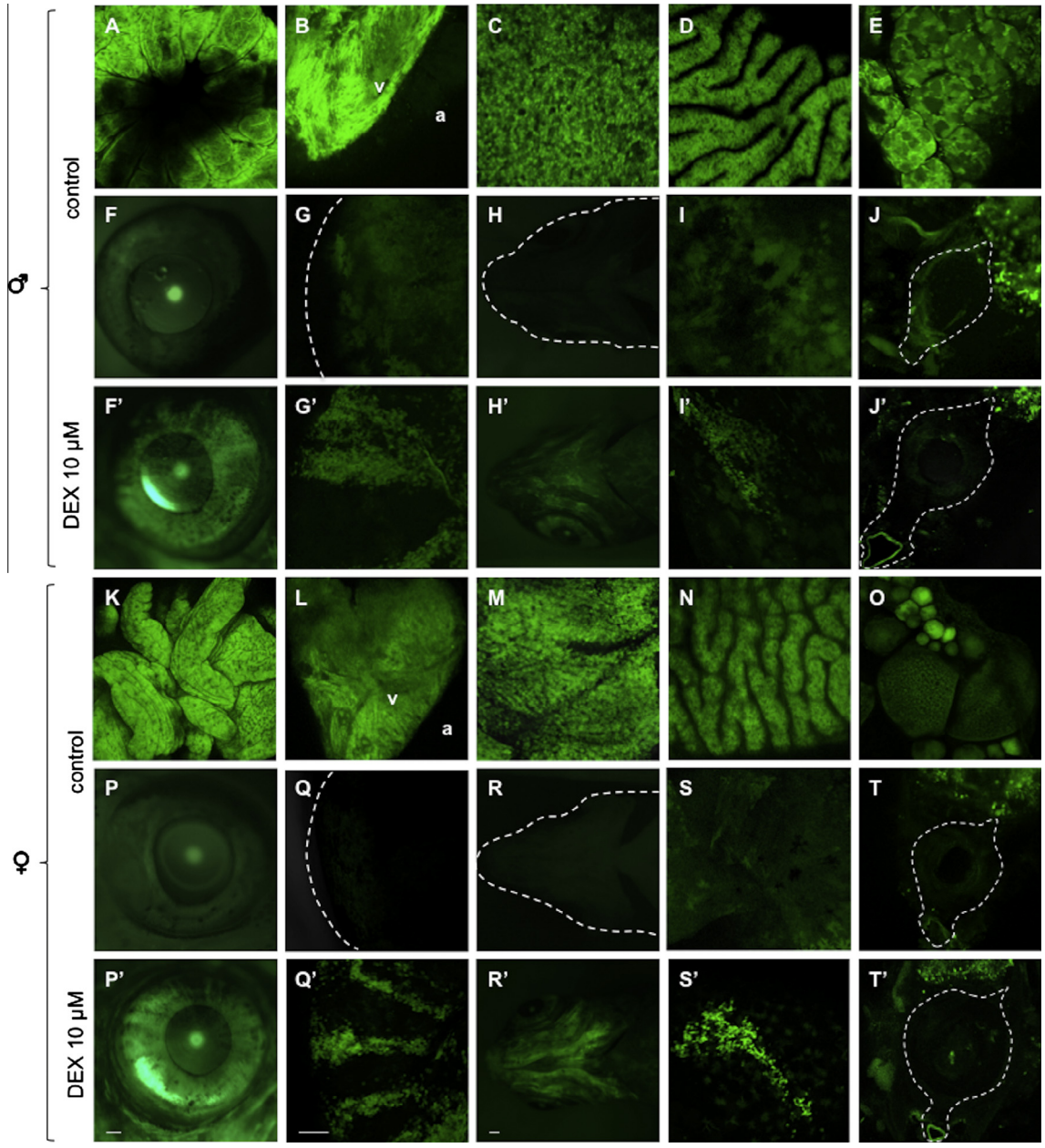

Fig. 7. 20× Confocal microscopy pictures showing EGFP in control and 10 µM DEX-treated adult zebrafish males and females: esophageal sacs (A and K), ventricular epicardium (B and L; *v* = ventricle; *a* = atrium), liver (C and M), intestinal mucosa (D and N), testis (E), ovary (O), eye (F and G, F′ and G′; P and Q, P′ and Q′), skeletal elements of the splanchnocranium (H′, R′), skin (I, I′, S, S′) and spinal cord (J, J′, T, T′). Scale bar: 200 µM.

responsiveness also to AR, transgene activation in the testis of adult zebrafish could be related to androgen receptor present in Sertoli cells contacting spermatogonia (de Waal et al., 2008) as well as to the occurrence of PR in Leydig and Sertoli cells (Chen et al., 2010).

Albeit only *gr* mRNA is present at high concentrations in ovulated eggs and during early developmental stages (Pikulkaew et al., 2010), thus validating the relevance of GC transgene activation in embryogenesis, this does not hold at adulthood, when all steroid hormone pathways are operative. In order to rule out potential modulation of the reporter by other steroid hormones in adult stage, specific mutant lines for the different GRE-sharing steroid receptors should be adopted.

The paternally acquired transgene was transcribed in the progeny already at 2 hpf, which is strikingly precocious, being timed at the cleavage stage, when the synchronous divisions of the blastomeres every 14–15 min limit the window for zygotic transcription (Tadros and Lipshitz, 2009). The embryonic content of *egfp* mRNA increased at 3 hpf with mid-blastula transition and remained high from 4 hpf onwards. The very early activation of the transgene promoter points to a fundamental developmental role of GCs and their receptor in zebrafish ontogenesis, as previously speculated (Pikulkaew et al., 2011). As reported in the Introduction, this observation contrast with the viability of the mutant zebrafish strain, s357gr−/−, that has been recently identified (Ziv et al., 2013). The R443C mutant Gr protein of this line can bind cortisol but cannot perform DNA binding activity due to a missense mutation located in the DNA-binding domain (Ziv et al., 2013) that impairs both transactivation and trans-repression. Although off-target effects have been excluded by co-injection of p53-MO, we cannot rule out that some developmental defects as well as the reduced viability of the gr-morphants could be partially ascribed

Please cite this article in press as: Benato, F., et al. A living biosensor model to dynamically trace glucocorticoid transcriptional activity during development and adult life in zebrafish. Molecular and Cellular Endocrinology (2014), http://dx.doi.org/10.1016/j.mce.2014.04.015

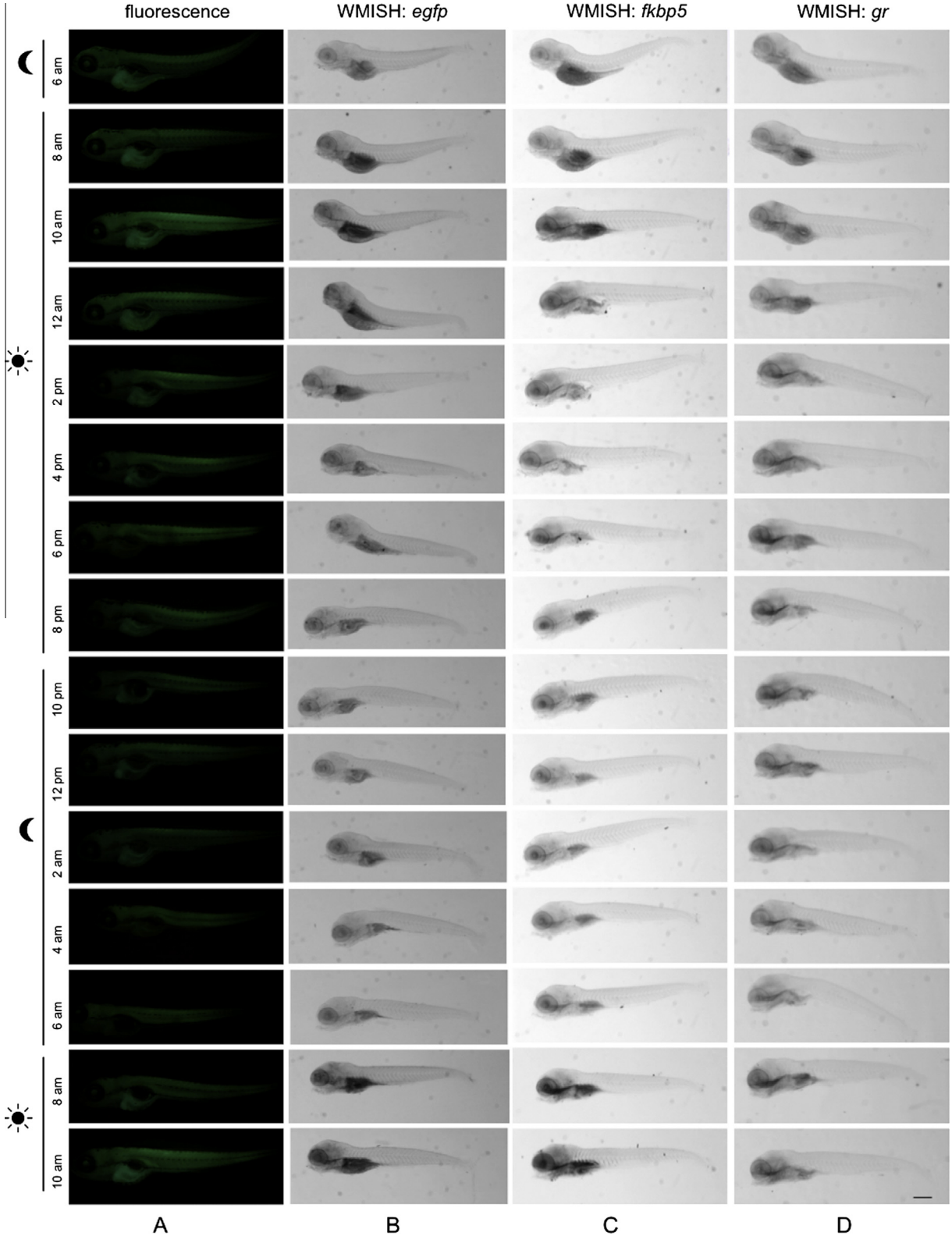

Fig. 8. (A) Fluorescence microscopy lateral view, (B) WMISH of *egfp* mRNA of 5-dpf transgenic larvae and (C) WMISH of *fkpb5* mRNA, (D) WMISH of *gr* mRNA of 5-dpf WT larvae exposed to standard photoperiodic regime and analyzed from 2 h before light onset for 28 h. Scale bar: 200 μM.

to this problem. However, in mouse a complete inactivation of the glucocorticoid receptor has been demonstrated to be inconsistent with life as $GR^{null/null}$ mice die just after birth (Cole et al., 1995). In contrast, mice carrying the $GR^{dim/dim}$ (Reichardt et al., 1998), that impairs homodimerization and DNA binding of the receptor (A458T), are viable. In these mutants the GRE-dependent gene transcription is absent whereas other DNA-binding independent activities of the GR receptor, such as cross-talk with other transcription factors are allowed. Thus, we can speculate that, in zebrafish gr R443C mutants, similarly to the corresponding human

Please cite this article in press as: Benato, F., et al. A living biosensor model to dynamically trace glucocorticoid transcriptional activity during development and adult life in zebrafish. Molecular and Cellular Endocrinology (2014), http://dx.doi.org/10.1016/j.mce.2014.04.015

GR R477H mutant that maintains full capacity to repress TNFα-induced NF-kB activity, some genomic functions are still present (Ruiz et al., 2013).

Our results suggest that the GC signaling pathway exerts a basic integrative function by targeting genes that confer priority for resource access and consumption. Specifically, during embryonic and larval development, EGFP was expressed in organs and body parts undergoing fast proliferation and differentiation, like head, tail, fins and primitive intestine with its hepatic and pancreatic offshoots.

In the ia20 line fluorescence was also precociously detected in fast developing sensory organs, like the eyes, the olfactory bulbs and tracts, and in other structures such as otic vesicles, pituitary and epiphysis. Energy allocation to these structures is justified by the immediate need of the larva to scan and process environmental cues into adaptive responses.

Furthermore, the role of activated GR in timing resource assignment is supported by the responses in terms of *egfp* transcript and protein disclosed by WMISH and fluorescence analysis in larvae exposed to standard photoperiodic regime as well as *fkbp5* expression. The trend of EGFP expression and its prevalent gastro-intestinal localization are interpretable as a functional predisposition for food seizing and digestion after nighttime fasting. GC signaling appears to harmonize the metabolic pre-activation of those organs that are expected to be soon functionally active, possibly by entraining local clocks. This hypothesis may be supported by the well-known surge in HPA axis activity before awakening in humans and other mammals (Chung et al., 2011). Of interest is the report that circadian cell proliferation rhythms were severely compromised by shutting down GC signaling in mutant zebrafish larvae with corticotrope deficiency (Dickmeis et al., 2007). Moreover, in mammals, regulation of a large proportion of the hepatic circadian transcriptome by GC signaling has been recently reported (Reddy et al., 2007).

In conclusion, although transgene activation in well-known GC targets, such as liver, bone, muscle or brain was expected, positivity in other structures, like olfactory complex, otic vesicles or putative KA″ cells, was actually a novelty. These results illustrate the potential of this transgenic line for deepening knowledge on GC functions during both development and adult life.

Acknowledgements

The authors wish to thank L. Pivotti and Dr. M. Milanetto for their valuable assistance in the fish facility. This work was kindly supported by EU Grant ZF-HEALTH CT-2010-242048, AIRC IG10274, CARIPARO 2009-2010 Projects, and PRIN 2010-2011 (2010W87LBJ) from the Ministry of the University and Scientific and Technological Research of Italy.

Appendix A. Supplementary material

Supplementary data associated with this article can be found, in the online version, at http://dx.doi.org/10.1016/j.mce.2014.04.015.

References

Adler, A.J., Danielsen, M., Robins, D.M., 1992. Androgen-specific gene activation via a consensus glucocorticoid response element is determined by interaction with nonreceptor factors. Proc. Nat. Acad. Sci. USA 89, 11660–11663.

Alsop, D., Vijayan, M.M., 2008. Development of the corticosteroid stress axis and receptor expression in zebrafish. Am. J. Physiol. – Regul., Integrative Comp. Physiol. 294, R711–R719.

Beildeck, M.E., Gelmann, E.P., Byers, S.W., 2010. Cross-regulation of signaling pathways: an example of nuclear hormone receptors and the canonical Wnt pathway. Exp. Cell Res. 316, 1763–1772.

Bury, N.R., Sturm, A., 2007. Evolution of the corticosteroid receptor signalling pathway in fish. Gen. Comp. Endocrinolol. 153, 47–56.

Chen, S.X., Bogerd, J., García-López, A., de Jonge, H., de Waal, P.P., Hong, W.S., Schulz, R.W., 2010. Molecular cloning and functional characterization of a zebrafish nuclear progesterone receptor. Biololy Reprod. 82, 171–181.

Chrousos, G.P., Kino, T., 2009. Glucocorticoid signaling in the cell expanding clinical implications to complex human behavioral and somatic disorders. Ann. N. Y. Acad. Sci. 1179, 153–166.

Chung, S., Son, G.H., Kim, K., 2011. Circadian rhythm of adrenal glucocorticoid: its regulation and clinical implications. Biochim. Biophys. Acta 1812, 581–591.

Cole, T.J., Blendy, J.A., Monaghan, A.P., Krieglstein, K., Schmid, W., Aguzzi, A., Fantuzzi, G., Hummler, E., Unsicker, K., Schutz, G., 1995. Targeted disruption of the glucocorticoid receptor gene blocks adrenergic chromaffin cell development and severely retards lung maturation. Genes Dev. 9, 1608–1621.

Corallo, D., Schiavinato, A., Trapani, V., Moro, E., Argenton, F., Bonaldo, P., 2013. Emilin3 is required for notochord sheath integrity and interacts with Scube2 to regulate notochord-derived Hedgehog signals. Development 140, 4594–4601.

De, P., Roy, S.G., Kar, D., Bandyopadhyay, A., 2011. Excess of glucocorticoid induces myocardial remodeling and alteration of calcium signaling in cardiomyocytes. J. Endocrinol. 209, 105–114.

de Waal, P.P., Wang, D.S., Nijenhuis, W.A., Schulz, R.W., Bogerd, J., 2008. Functional characterization and expression analysis of the androgen receptor in zebrafish (*Danio rerio*) testis. Reproduction 136, 225–234.

Dickmeis, T., Lahiri, K., Nica, G., Vallone, D., Syantoriello, C., Neumann, C.J., Hammerschmidt, M., Foulkes, N.S., 2007. Glucocorticoids play a key role in circadian cell cycle rhythms. PLoS Biol. 5, e78.

Foligne, B., Aissaoui, S., Senegas-Balas, F., Cayuela, C., Bernard, P., Antoine, J.M., Balas, D., 2001. Changes in cell proliferation and differentiation of adult rat small intestine epithelium after adrenalectomy: kinetic, biochemical, and morphological studies. Dig. Dis. Sci. 46, 1236–1246.

Gorelick, D.A., Halpern, M.E., 2011. Visualization of estrogen receptor transcriptional activation in zebrafish. Endocrinology 152, 2690–2703.

Grange, T., Roux, J., Rigaud, G., Pictet, R., 1991. Cell-type specific activity of two glucocorticoid responsive units of rat *tyrosine aminotransferase* gene is associated with multiple binding sites for C/EBP and a novel liver-specific nuclear factor. Nucleic Acids Res. 19, 131–139.

Griffith, B.B., Schoonheim, P.J., Ziv, L., Voelker, L., Baier, H., Gahtan, E., 2012. A zebrafish model of glucocorticoid resistance shows serotonergic modulation of the stress response. Frontiers Behavioral Neurosci. 6, 68. http://dx.doi.org/10.3389/fnbeh.2012.00068.

Gross, K.L., Cidlowski, J.A., 2008. Tissue-specific glucocorticoid action: a family affair. Trends Endocrinol. Metab. 19, 331–339.

Hanna, R.N., Daly, S.C., Pang, Y., Anglade, I., Kah, O., Thomas, P., Zhu, Y., 2010. Characterization and expression of the nuclear progestin receptor in zebrafish gonads and brain. Biol. Reprod. 82, 112–122.

Hoffman, R.M., 2008. Use of GFP for *in vivo* imaging: concepts and misconceptions. Proc. SPIE 6868, 68680E–68685E.

Huang, P., Xiong, F., Megason, S.G., Schier, A.F., 2012. Attenuation of Notch and Hedgehog signaling is required for fate specification in the spinal cord. PLoS Genet. 8, e1002762.

Jääskeläinen, T., Makkonen, H., Palvimo, J.J., 2011. Steroid up-regulation of FKBP51 and its role in hormone signaling. Curr. Opin. Pharmacol. 11, 326–331.

Jantzen, H.M., Strähle, U., Gloss, B., Stewart, F., Schmid, W., Boshart, M., Miksicek, R., Schütz, G., 1987. Cooperativity of glucocorticoid response elements located far upstream of the *tyrosine aminotransferase* gene. Cell 49, 29–38.

Kassel, O., Herrlich, P., 2007. Crosstalk between the glucocorticoid receptor and other transcription factors: molecular aspects. Mol. Cell. Endocrinol. 275, 13–29.

Kawakami, K., 2007. Tol2: a versatile gene transfer vector in vertebrates. Genome Biol. 1, S7.

Kawakami, K., Takeda, H., Kawakami, N., Kobayashi, M., Matsuda, N., Mishina, M., 2004. A transposon-mediated gene trap approach identifies developmentally regulated genes in zebrafish. Dev. Cell 7, 133–144.

Kimmel, C.B., Ballard, W.W., Kimme, l S.R., Ullmann, B., Schilling, T.F., 1995. Stages of embryonic development in the zebrafish. Dev. Dyn. 203, 253–310.

Koubovec, D., Ronacher, K., Stubsrud, E., Louw, A., Hapgood, J.P., 2005. Synthetic progestins used in HRT have different glucocorticoid agonist properties. Mol. Cell. Endocrinol. 242, 23–32.

Kwan, K.M., Fujimoto, E., Grabher, C., Mangum, B.D., Hardy, M.E., Campbell, D.S., Parant, J.M., Yost, H.J., Kanki, J.P., Chien, C.B., 2007. The Tol2kit: a multisite gateway-based construction kit for Tol2 transposon transgenesis constructs. Dev. Dyn. 236, 3088–3099.

Laux, D.W., Febbo, J.A., Roman, B.L., 2011. Dynamic analysis of BMP-responsive smad activity in live zebrafish embryos. Dev. Dyn. 240, 682–694.

Leatherland, J.F., Li, M., Barkataki, S., 2010. Stressors, glucocorticoids and ovarian function in teleosts. J. Fish Biol. 76, 86–111.

Merkulov, V.M., Merkulova, T.I., 2009. Structural variants of glucocorticoid receptor binding sites and different versions of positive glucocorticoid responsive elements: analysis of GR-TRRD database. J. Steroid Biochem. Mol. Biol. 115, 1–8.

Moro, E., Gnügge, L., Braghetta, P., Bortolussi, M., Argenton, F., 2009. Analysis of beta cell proliferation dynamics in zebrafish. Dev. Biol. 332, 299–308.

Moro, E., Ozhan-Kizil, G., Mongera, A., Beis, D., Wierzbicki, C., Young, R.M., Bournele, D., Domenichini, A., Valdivia, L.E., Lum, L., Chen, C., Amatruda, J.F., Tiso, N., Weidinger, G., Argenton, F., 2012. *In vivo* Wnt signaling tracing through a transgenic biosensor fish reveals novel activity domains. Dev. Biol. 366, 327–340.

UNCORRECTED PROOF

Mueller, M., Atanasov, A., Cima, I., Corazza, N., Schoonjans, K., Brunner, T., 2007. Differential regulation of glucocorticoid synthesis in murine intestinal epithelial versus adrenocortical cell lines. Endocrinology 148, 1445–1453.

Nesan, D., Vijayan, M.M., 2013. Role of glucocorticoid in developmental programming: evidence from zebrafish. Gen. Comp. Endocrinol. 181, 35–44.

Nesan, D., Kamkar, M., Burrows, J., Scott, I.C., Marsden, M., Vijayan, M.M., 2012. Glucocorticoid receptor signaling is essential for mesoderm formation and muscle development in zebrafish. Endocrinology 153, 1288–1300.

Parajes, S., Griffin, A., Taylor, A.E., Rose, I.T., Miguel-Escalada, I., Hadzhiev, Y., Arlt, W., Shackleton, C., Müller, F., Krone, N., 2013. Redefining the initiation and maintenance of zebrafish interrenal steroidogenesis by characterizing the key enzyme Cyp11a2. Endocrinology 154, 2702–2711.

Pfaffl, M.W., 2009. Rest 2009 Software User Guide. Qiagen, Hilden, Germany.

Pfaffl, M.W., Horgan, G.W., Dempfle, L., 2002. Relative expression software tool (REST) for group-wise comparison and statistical analysis of relative expression results in real-time PCR. Nucleic Acids Res. 30, e36.

Pikulkaew, S., De Nadai, A., Belvedere, P., Colombo, L., Dalla Valle, L., 2010. Expression analysis of steroid hormone receptor mRNAs during zebrafish embryogenesis. Gen. Comp. Endocrinol. 165, 215–220.

Pikulkaew, S., Benato, F., Celeghin, A., Zucal, C., Skobo, T., Colombo, L., Dalla Valle, L., 2011. The knockdown of maternal glucocorticoid receptor mRNA alters embryo development in zebrafish. Dev. Dyn. 240, 874–889.

Pujols, L., Mullol, J., Roca-Ferrer, J., Torrego, A., Xaubet, A., Cidlowski, J.A., Picado, C., 2002. Expression of glucocorticoid receptor α- and β-isoforms in human cells and tissues. Am. J. Physiol. – Cell Physiol. 283, C1324–C1331.

Quaroni, A., Tian, J.Q., Göke, M., Podolsky, D.K., 1999. Glucocorticoids have pleiotropic effects on small intestinal crypt cells. Am. J. Physiol. 277, G1027–G1040.

Rae, M.T., Niven, D., Critchley, H.O., Harlow, C.R., Hillier, S.G., 2004. Anti inflammatory steroid action in human ovarian surface epithelial cells. J. Clin. Endocrinol. Metab. 89, 4538–4544.

Reddy, A.B., Maywood, E.S., Karp, N.A., King, V.M., Inoue, Y., Gonzalez, F.J., Lilley, K.S., Kyriacou, C.P., Hastings, M.H., 2007. Glucocorticoid signaling synchronizes the liver circadian transcriptome. Hepatology 45, 1478–1488.

Reichardt, H.M., Kaestner, K.H., Tuckermann, J., Kretz, O., Wessely, O., Bock, R., Gass, P., Schmid, W., Herrlich, P., Angel, P., Schütz, G., 1998. DNA binding of the glucocorticoid receptor is not essential for survival. Cell 93, 531–541.

Ren, R., Oakley, R.H., Cruz-Topete, D., Cidlowski, J.A., 2012. Dual role for glucocorticoids in cardiomyocyte hypertrophy and apoptosis. Endocrinology 153, 5346–5360.

Rog-Zielinska, E.A., Thomson, A., Kenyon, C.J., Brownstein, D.G., Moran, C.M., Szumska, D., Michailidou, Z., Richardson, J., Owen, E., Watt, A., Morrison, H., Forrester, L.M., Bhattacharya, S., Holmes, M.C., Chapman, K.E., 2013. Glucocorticoid receptor is required for foetal heart maturation. Hum. Mol. Genet. 22, 3269–3282.

Rose, A.J., Vegiopoulos, A., Herzig, S., 2010. Role of glucocorticoids and the glucocorticoid receptor in metabolism: insights from genetic manipulations. J. Steroid Biochem. Mol. Biol. 122, 10–20.

Ruiz, M., Hedman, E., Gåfvels, M., Eggertsen, G., Werner, S., Wahrenberg, H., Wikström, A.C., 2013. Further characterization of human glucocorticoid receptor mutants, R477H and G679S, associated with primary generalized glucocorticoid resistance. Scand. J. Clin. Lab. Invest. 73, 203–207.

Sainte-Marie, Y., Nguyen Dinh Cat, A., Perrier, R., Mangin, L., Soukaseum, C., Peuchmaur, M., Tronche, F., Farman, N., Escoubet, B., Benitah, J.P., Jaisser, F., 2007. Conditional glucocorticoid receptor expression in the heart induces atrio-ventricular block. FASEB J. 21, 3133–3141.

Sapolsky, R.M., Romero, L.M., Munck, A.U., 2000. How do glucocorticoids influence stress responses? Integrating permissive, suppressive, stimulatory, and preparative actions. Endocr. Rev. 21, 55–89.

Schoneveld, O.J., Gaemers, I.C., Lamers, W.H., 2004. Mechanisms of glucocorticoid signaling. Biochim. Biophys. Acta 1680, 114–128.

Schwend, T., Loucks, E.J., Ahlgren, S.C., 2010. Visualization of Gli activity in craniofacial tissues of hedgehog-pathway reporter transgenic zebrafish. PLoS ONE 5, e14396.

Selman, P.J., Wolfswinkel, J., Mol, J.A., 1996. Binding specificity of medroxyprogesterone acetate and proligestone for the progesterone and glucocorticoid receptor in the dog. Steroids 61, 133–137.

Tadros, W., Lipshitz, H.D., 2009. The maternal-to-zygotic transition: a play in two acts. Development 136, 3033–3042.

Takagi, C., Takahashi, H., Kudose, H., Kato, K., Sakamoto, T., 2011. Dual in vitro effects of cortisol on cell turnover in the medaka esophagus via the glucocorticoid receptor. Life Sci. 88, 239–245.

Tetsuka, M., Milne, M., Simpson, G.E., Hillier, S.G., 1999. Expression of 11b-hydroxysteroid dehydrogenase, glucocorticoid receptor and mineralocorticoid receptor genes in rat ovary. Biol. Reprod. 60, 330–335.

Thisse, C., Thisse, B., 2008. High-resolution *in situ* hybridization to whole-mount zebrafish embryos. Nat. Protoc. 3, 59–69.

Wang, J.M., Préfontaine, G.G., Lemieux, M.E., Pope, L., Akimenko, M.A., Haché, R.J., 1999. Developmental effects of ectopic expression of the glucocorticoid receptor DNA binding domain are alleviated by an amino acid substitution that interferes with homeodomain binding. Mol. Cell. Biol. 19, 7106–7122.

Weger, B.D., Weger, M., Nusser, M., Brenner-Weiss, G., Dickmeis, T., 2012. A chemical screening system for glucocorticoid stress hormone signaling in an intact vertebrate. ACS Chem. Biol. 7, 1178–1183.

Westerfield, M., 1995. The Zebrafish Book. University of Oregon Press, Eugene.

Zhou, H., Mak, W., Kalak, R., Street, J., Fong-Yee, C., Zheng, Y., Dunstan, C.R., Seibel, M.J., 2009. Glucocorticoid-dependent Wnt signaling by mature osteoblasts is a key regulator of cranial skeletal development in mice. Development 136, 427–436.

Ziv, L., Muto, A., Schoonheim, P.J., Meijsing, S.H., Strasser, D., Ingraham, H.A., Schaaf, M.J.M., Yamamoto, K.R., Baier, H., 2013. An affective disorder in zebrafish with mutation of the glucocorticoid receptor. Mol. Psychiatry 18, 681–689.

UNCORRECTED PROOF

Please cite this article in press as: Benato, F., et al. A living biosensor model to dynamically trace glucocorticoid transcriptional activity during development and adult life in zebrafish. Molecular and Cellular Endocrinology (2014), http://dx.doi.org/10.1016/j.mce.2014.04.015